

Optical Resolution of Aromatic Alcohols Using Silica Nanoparticles Grafted with Helicene

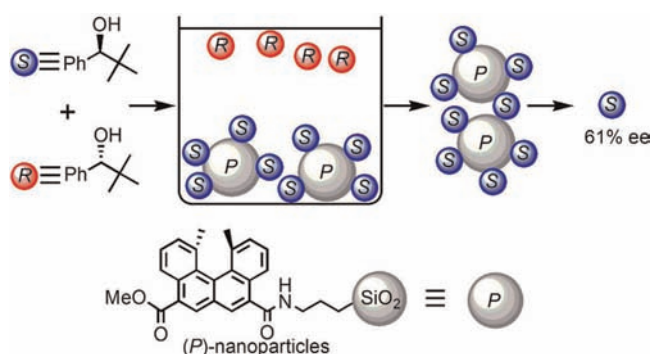
Wataru Ichinose, Masamichi Miyagawa, Zengjian An, and Masahiko Yamaguchi*

Department of Organic Chemistry, Graduate School of Pharmaceutical Sciences,
Tohoku University, Aoba, Sendai 980-8578, Japan

yama@m.tohoku.ac.jp

Received May 2, 2012

ABSTRACT



Optically active silica nanoparticles, with a 70-nm diameter, grafted with (*P*)-1,12-dimethyl-8-methoxycarbonylbenzo[*c*]phenanthrene-5-carboxamide were synthesized, and their use in the kinetic resolution of aromatic alcohols was examined. Up to 61% ee for (*S*)-2,2-dimethyl-1-phenyl-1-propanol was obtained by a preferential precipitation of aggregates formed with (*P*)-nanoparticles.

Racemic organic compounds have been resolved by recrystallizing diastereomeric salts, typically those derived from 1:1 mixtures of carboxylic acids and amines, employing diastereomers with different solubilities.¹ The method, however, cannot be applied to nonpolar organic compounds, which do not readily crystallize. In such cases, chiral high performance liquid chromatography (HPLC) separation has been conducted, which requires several pieces of equipment.² Other methods such as co-crystallization^{3,4} and polymer imprinting^{5–7} were also

developed, although they were not quite common. In this study, the use of optically active nanoparticles for the resolution of aromatic alcohols by a preferential aggregation and precipitation of an enantiomer is described. This method can be used for the resolution of nonpolar non-crystalline compounds and has an advantage of using smaller molar amounts of the resolving reagent compared to racemic compounds. Although studies have been conducted for the resolution of racemic acids or amino acid derivatives with chiral nanoparticles,^{8–10} there are as yet no studies of nonpolar alcohols.¹¹

3-Aminopropylated silica nanoparticles¹² (2.3 mmol/g) of 70-nm mean diameter were grafted with (*P*)-1,

(1) Recent review: Faigal, F.; Forgassy, E.; Nogradi, M.; Palovics, E.; Schindler, J. *Tetrahedron: Asymmetry* **2008**, *19*, 519–536.

(2) Recent review: Okamoto, Y.; Ikai, T. *Chem. Soc. Rev.* **2008**, *37*, 2593–2608.

(3) Kobayashi, Y.; Kodama, K.; Saigo, K. *Org. Lett.* **2004**, *6*, 2941–2944.

(4) Toda, F.; Tanaka, K.; Matsumoto, T.; Nakai, T.; Miyahara, I.; Hirotsu, K. *J. Phys. Org. Chem.* **2000**, *13*, 39–45.

(5) Nakano, T.; Satoh, Y.; Okamoto, Y. *Macromolecules* **2001**, *34*, 2405–2407.

(6) Teraguchi, M.; Suzuki, J.; Kaneko, T.; Aoki, T.; Masuda, T. *Macromolecules* **2003**, *36*, 9694–9697.

(7) Ryoo, J. J.; Shin, J. W.; Dho, H. S.; Min, K. S. *Inorg. Chem.* **2010**, *49*, 7232–7234.

(8) Choi, H. J.; Hyun, M. H. *Chem. Commun.* **2009**, 6454–6456.

(9) Chen, X.; Rao, J.; Wang, J.; Gooding, J. J.; Zou, G.; Zhang, Q. *Chem. Commun.* **2011**, *47*, 10317–10319.

(10) Xu, W.; Cheng, Z.; Zhang, L.; Zhang, Z.; Zhu, J.; Zhou, N.; Zhu, X. *J. Polym. Sci., Part A: Polym. Chem.* **2010**, *48*, 1324–1331.

(11) The enantioselective interaction of chiral gold nanoparticles with propylene oxide was examined. Shukla, N.; Bartel, M. A.; Gellman, A. J. *J. Am. Chem. Soc.* **2010**, *132*, 8575–8580.

(12) Rahman, I. A.; Jafarzadeh, M.; Sipaut, C. S. *Ceram. Int.* **2009**, *35*, 1883–1888.

12-dimethyl-8-methoxycarbonylbenzo[*c*]phenanthrene-5-carboxylic acid chloride by treating them in refluxing isopropyl ether for 4 h in the presence of ethyldiisopropylamine. The grafted chiral (*P*)-nanoparticles were stored in ethanol, and IR, CD, UV–vis, and thermogravimetry (TG) analyses were conducted (Figures S2, S4, S5). A loading amount of 0.15 mmol/g was obtained by CD, UV–vis, and elemental analyses (Figure S5). No irreversible aggregation was observed during grafting, as indicated by the results of the dynamic light scattering (DLS) and atomic force microscopy (AFM) analyses (Figures S6, S7). The nanoparticles were stable in ethanol for 72 h, as indicated by the results of the DLS analysis, and sonication did not affect the dispersed state (Figure S7).

Reversible aggregate formation was observed for the 70-nm-diameter silica (*P*)-nanoparticles in different solvents as well as for the 210 nm particles reported before.¹³ The (*P*)-nanoparticles in ethanol (20 mg/20 mL) were centrifuged, and the collected nanoparticles were mixed with trifluoromethylbenzene (20 mL). The aggregated particles of 3100-nm mean diameter were formed as indicated by the results of the DLS analysis. When the aggregated nanoparticles were mixed with iodobenzene, smaller aggregates of 220-nm mean diameter were formed. Mixing with chlorobenzene gave 620-nm-diameter aggregates, whereas mixing with toluene gave 1300-nm-diameter aggregates. The solvent exchange of (*P*)-nanoparticles in iodobenzene to trifluoromethylbenzene changed the diameter of the aggregated particles from 220 to 2700 nm. The (*P*)-nanoparticles were dispersed in soft aromatic solvents and reversibly aggregated in hard solvents (Figure S3).

A notable observation was made when (*P*)-nanoparticles were mixed with optically pure 1-phenylethanol **1**. A mixture of (*P*)-nanoparticles (1.0 mg) and (*S*)-**1** (0.18 mg) was dispersed in *m*-bis(trifluoromethyl)benzene (0.2 mL) and was allowed to settle at room temperature (Figure 1). Precipitates started to form after 7 h and were completed after 12 h. The observation is in contrast to that of (*R*)-**1**, which started to precipitate after 18 h and was completed after 26 h. Without **1**, (*P*)-nanoparticles started to precipitate only after 42 h in the same solvent. The higher tendency of (*S*)-**1** to form precipitates was ascribed to the stronger interactions of (*S*)-**1** and (*P*)-nanoparticles compared to (*R*)-**1**, which is a chiral recognition phenomenon in the interactions of chiral nanoparticles with small chiral molecules. Both (*S*)-**1** and (*R*)-**1** formed similar aggregates of 800-nm mean size at the start of the precipitation, as indicated by the results of the AFM analysis (Figure S8).

The mechanism of precipitation and chiral recognition was examined. The (*P*)-nanoparticles were washed with triethylamine and dispersed in *m*-bis(trifluoromethyl)benzene. When (*S*)-**1** or (*R*)-**1** was added, each solution formed a precipitate within 10 min. In contrast, (*P*)-nanoparticles washed with trifluoroacetic acid began precipitation with

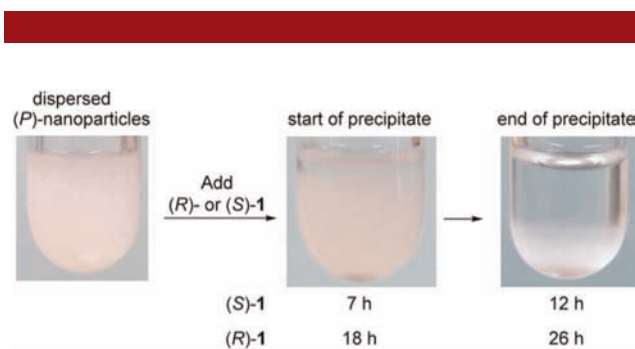


Figure 1. Enantioselective precipitation of **1** (0.18 mg) by (*P*)-nanoparticles (1.0 mg) in *m*-bis(trifluoromethyl)benzene (0.2 mL) at 25 °C.

(*S*)-**1** in 14 h and completed in 24 h; precipitation with (*R*)-**1** started at 24 h and completed in 36 h. These results indicated that the amine groups on the surface were protonated,¹⁴ and electrostatic repulsions between the positive charges on the surface inhibited the aggregation of nanoparticles (Figure 2). The adsorption of **1** on the surfaces reduced the electrostatic repulsions and prompted aggregation, during which process chiral recognition occurred. It may be consistent with the experimental results that (*P*)-nanoparticles contained 2.3 mmol/g amines and 0.15 mmol/g (*P*)-helicene.

On the basis of our observations, optical resolution was examined. To a mixture of (*P*)-nanoparticles (20 mg) in *m*-bis(trifluoromethyl)benzene (4 mL), (\pm)-**1** (3.6 mg) was added, and the mixture was allowed to settle for 12 h. The precipitate was separated by centrifugation and mixed with 2-propanol (1 mL). After insoluble materials were removed by centrifugation, the solution was concentrated, and (*S*)-**1** was obtained in 18% yield (maximum yield of 50%), as indicated by the results of the UV–vis analysis

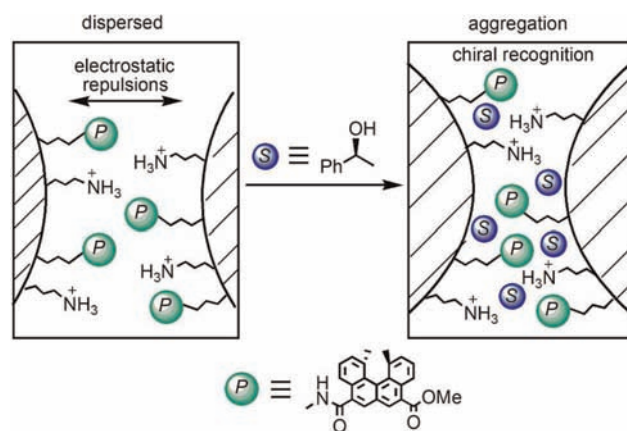


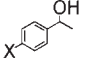
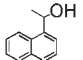
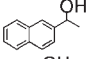
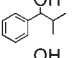
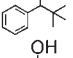
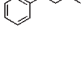
Figure 2. Possible mechanism of aggregation.

and in 47% ee as indicated by those of the HPLC analysis. From the supernatant, (*R*)-**1** was recovered in 70% yield

(13) An, Z.; Yasui, Y.; Togashi, T.; Adschiri, T.; Hitosugi, S.; Isobe, H.; Higuchi, T.; Shimomura, M.; Yamaguchi, M. *Chem. Lett.* **2010**, *39*, 1004–1005. Chiral recognition in aggregation of gold nanoparticles grafted with helicenes was examined. An, Z.; Yamaguchi, M. *Chem. Commun.*, submitted.

(14) Wu, Z.; Xiang, H.; Kim, T.; Chun, S. M.; Lee, K. *J. Colloid Interface Sci.* **2006**, *304*, 119–124.

Table 1. Optical Resolutions of Aromatic Alcohols
(See Supporting Information for Experimental Detail)

alcohol	% ee ^a	yield(%) ^b	absolute configuration ^c	
	X = F	35	17	(S)
	X = Cl	32	16	
	X = H	47	18	(S)
	X = Me	35	17	
	X = OMe	29	18	(S)
		36	19	
		39	20	(S)
		52	18	(S)
		61	14	(S)
		55	15	(S)

^a Enantiomeric excess values were determined by HPLC. ^b Yields were determined by HPLC. ^c Absolute configurations of alcohols were determined by the order of elution in HPLC.^{3,15}

with 3% ee. The reaction time was critical, and treatment for 9 and 18 h gave (*S*)-**1** in 11% ee (5% yield) and 19% ee (19% yield), respectively. An intermediate period of 12 h between the start of precipitation for (*S*)-**1** and (*R*)-**1** was employed. The (*P*)-nanoparticles could be reused, and use of recovered (*P*)-nanoparticles provided (*S*)-**1** in 44% ee (11% yield). Preparative resolution was conducted using (\pm)-**1** (36 mg) and (*P*)-nanoparticles (200 mg), and (*S*)-**1** (5.1 mg, 14%, 44% ee) was obtained.

The above procedures employed 10 equiv of (\pm)-**1** based on (*P*)-helicene on a silica surface. An intriguing aspect of the nanoparticle resolution method is that an excess amount of a racemic substrate can be used over the resolving reagent. When 1 equiv of (\pm)-**1** was employed, (*S*)-**1** was obtained in 35% yield with 53% ee. (*S*)-**1** was obtained in 18% yield with 29% ee even with the use of 20 equiv of (\pm)-**1**. The stoichiometries of (\pm)-**1** and (*P*)-nanoparticles have relatively small effects on the efficiency of resolution.

Precipitation analysis could be conveniently used for the optimization of conditions, as indicated in the examination

(15) Yamamoto, Y.; Shirai, T.; Watanabe, M.; Kurihara, K.; Miyaura, N. *Molecules* **2011**, *16*, 5020–5034.

of the solvent effect. The time of the start of precipitation was examined for (*R*)-**1** and (*S*)-**1** in various solvents. In all the solvents, (*S*)-**1** precipitated faster than (*R*)-**1**, and the ratios of the time are summarized in Table S1. Notably, the ratio showed good correlation with the enantiomeric excess of (*S*)-**1** obtained by the resolution of (\pm)-**1**. The results indicate the kinetic nature of this resolution method. In general, the fluorine-containing benzenes showed higher enantiomeric excesses of (*S*)-**1**: CF₃C₆H₅, 40% ee; *p*-(CF₃)₂-C₆H₄, 34% ee; *m*-F₂C₆H₄, 30% ee; FC₆H₅, 29% ee. Polar solvents such as DMSO, NMP, THF, CH₃CN, EtOH, morpholine, and AcOEt showed selectivities below 25% ee.

The substituent effect on aromatic alcohols was examined (Table 1). Bulkier alkyl derivatives showed high enantiomeric excesses, and 2-methyl-1-phenyl-1-propanol, 2,2-dimethyl-1-phenyl-1-propanol, and 1-phenyl-1-butanol gave 52% ee, 61% ee, and 55% ee, respectively. In contrast, a relatively small effect of the aromatic substituent was observed. (*p*-Fluorophenyl)-1-ethanol gave an (*S*)-isomer of 35% ee and (*p*-chlorophenyl)-1-ethanol gave an (*S*)-isomer of 32% ee.

To summarize, racemic aromatic alcohols were kinetically resolved using 70-nm-diameter optically active silica (*P*)-nanoparticles grafted with (*P*)-1,12-dimethyl-8-methoxycarbonylbenzo[*c*]phenanthrene-5-carboxamide, and up to 61% ee of the (*S*)-isomer was obtained. The different rates of precipitation between the enantiomers were exploited for the resolution, which could visually be monitored. This method can be used for the resolution of noncrystalline substances using a small nonstoichiometric amount of the resolving reagent.

Acknowledgment. Financial support from JSPS (No. 21229001) and G-COE is acknowledged. W.I. thanks the JSPS for a Fellowship for Young Japanese Scientists. We thank Professor Hiroyuki Isobe (Graduate School of Science, Tohoku University) for DLS use.

Supporting Information Available. Experimental procedures for synthesis of (*P*)-nanoparticles and optical resolution, CD and UV–vis spectra of (*P*)-nanoparticles, AFM images of the (*P*)-nanoparticles, TG, and DLS of (*P*)-nanoparticles. This material is available free of charge via the Internet at <http://pubs.acs.org>.

The authors declare no competing financial interest.